Defects and the optical absorption in nanocrystalline ZnO

2007 J. Phys.: Condens. Matter 19 236218

(http://iopscience.iop.org/0953-8984/19/23/236218)

IOP PUBLISHING JOURNAL OF PHYSICS: CONDENSED MATTER

J. Phys.: Condens. Matter **19** (2007) 236218 (11pp) doi:10.1088/0953-8984/19/23/236218

Defects and the optical absorption in nanocrystalline ZnO

Sreetama Dutta[1], Sanjay Chattopadhyay[2], Manas Sutradhar[3], Anindya Sarkar[4,6], Mahuya Chakrabarti[5], Dirtha Sanyal[5] and Debnarayan Jana[1]

[1] Department of Physics, University of Calcutta, 92 Acharya Prafulla Chandra Road, Kolkata 700 009, India
[2] Department of Physics, Taki Government College, Taki 743429, India
[3] Department of Chemistry, University of Calcutta, 92 Acharya Prafulla Chandra Road, Kolkata 700 009, India
[4] Department of Physics, Bangabasi Morning College, 19 Rajkumar Chakraborty Sarani, Kolkata 700 009, India
[5] Variable Energy Cyclotron Centre, 1/AF, Bidhannagar, Kolkata 700 064, India

E-mail: djphy@caluniv.ac.in

Received 13 February 2007, in final form 2 April 2007
Published 15 May 2007
Online at stacks.iop.org/JPhysCM/19/236218

Abstract

The correlation between the structural and optical properties of mechanically milled high purity ZnO powder is reported in the present work. Reduction of average grain size and enhancement of strain as a result of milling have been estimated from the broadening of x-ray powder diffraction patterns. After milling, the optical bandgap, revealed from absorption spectroscopy, has been red-shifted and the width of the localized states, calculated from the analysis of the Urbach tail below the absorption edge, has been extended more and more into the bandgap. Moreover, the band tailing parameter is seen to vary exponentially with the inverse of the grain size. Finally, the positron annihilation technique has been employed to identify the nature of defects present (or generated due to milling) in the system and thereby to correlate the defect mediated modification of optical absorption in ZnO.

(Some figures in this article are in colour only in the electronic version)

1. Introduction

Recently, zinc oxide (ZnO) has been a subject of research due to its unique opto-electronic properties [1], which can be employed in devices such as ultraviolet (UV) light-emitting diodes (LEDs), blue luminescent devices, UV lasers and gas sensors [2–4]. Besides, this system

[6] Presently on leave at: Dipartimento di Fisica, Università di Trento, Via Sommarie 14, 38050 Povo, Trento, Italy.

is being widely studied for a better understanding on some fundamentally interesting issues related to the optical, transport and magnetic properties of such wide bandgap semiconducting materials [5–7].

Magnetic nanoparticles have been a subject of intense research in the past decade because their fascinating magnetic character is very appealing in both theoretical as well as technological aspects [8]. Generally, materials with nanoscale dimensions show qualitative and quantitative changes in their electronic and optical properties compared to those of their bulk counterparts [9], and ZnO is not an exception [7, 10]. An in-depth understanding of the size-induced modification of material properties is necessary for ZnO like other semiconductor nanosystems. It is well known that lowering of grain size enhances the grain-surface region in the material. Such regions are defect rich [11] and the nature and abundance of these defect centres plays a crucial role in controlling the physical properties of ZnO [12–14]. Positron annihilation spectroscopy (PAS) [15, 16], one of the most powerful non-destructive techniques to characterize defects, is needed to probe the defect structure in ZnO, so purposeful engineering of defects to tune the material according to the technological need [17] becomes more and more prospective.

Recently, several techniques have been developed to fabricate nanocrystalline ZnO such as sputtering [18], pulse laser deposition [19], metal–organic chemical vapour deposition [20], oxidation of metallic zinc [21], molecular beam epitaxy [22], and the sol–gel process [23], each having their own advantages and limitations. As far as production of a large amount of homogeneous nanomaterial with lower cost and minimum chemical contamination is concerned, mechanical milling (or ball milling) is one of most effective methods to produce nanocrystalline semiconductors [24] including ZnO [10, 25]. In this paper, our aim is to characterize the defects and disorder in such a milled ZnO system and to study their role in optical absorption characteristics. A systematic study in this regard would be beneficial to understand similar types of systems in future.

2. Experimental details

As-supplied polycrystalline ZnO powder (purity 99.9% from Sigma-Aldrich, Germany) samples have been ball-milled (ball:mass = 10:1) by a Fritsch Pulverisette 6 planetary ball-mill grinder. The milling time has been varied from 1 to 32 h to achieve nanocrystalline ZnO of varying grain size. The x-ray diffraction (XRD) patterns of all the samples have been recorded in a Philips PW 1710 automatic diffractometer with Cu Kα radiation. In each case scanning has been performed in the range of 25°–80° (2θ) with a step size 0.02°. The average grain size of the powdered samples has been estimated from the conventional Scherer's formula [26]. The contribution of instrumental broadening has been taken into consideration.

The electronic absorption spectra of the ZnO samples have been recorded on a Hitachi U-3501 spectrophotometer in the wavelength range of 300–1100 nm.

Different sets of samples have been pressed into pellets ($\sim$1 mm thickness and 10 mm diameter) for positron annihilation spectroscopic investigation. The basic idea of Doppler broadening of the electron–positron annihilation radiation lineshape measurement can be found elsewhere [27–29]. For the coincidence Doppler broadening of the electron–positron annihilation γ-radiation (CDBEPAR) measurement two identical HPGe detectors (*efficiency* 12%; *type* PGC 1216sp of DSG, Germany) having energy resolution of 1.1 keV at 514 keV of ^{85}Sr have been used as two 511 keV γ-ray detectors, while the CDBEPAR spectra have been recorded in a dual ADC based–multiparameter data acquisition system (MPA-3 of FAST ComTec., Germany). The S parameter, calculated as the ratio of counts in the central area of the 511 keV photo-peak ($|511\ \text{keV} - E_\gamma| \leqslant 0.86$ keV) to the total area of the photo-peak

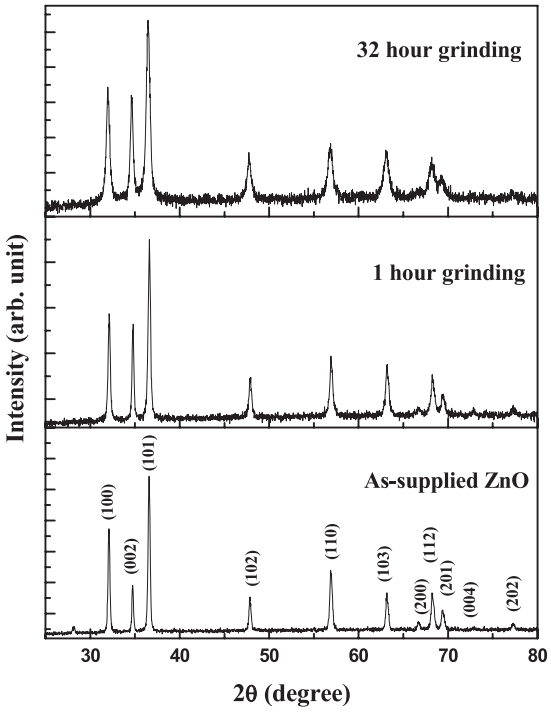

Figure 1. X-ray diffraction patterns for the as-supplied and nano-ZnO samples.

($|511\ \text{keV} - E_\gamma| \leqslant 4.25\ \text{keV}$), represents the fraction of positrons annihilating with the lower momentum electrons [16]. The W parameter, calculated as the ratio of counts in the wing region of the 511 keV photo-peak ($1.6\ \text{keV} \leqslant |E_\gamma - 511\ \text{keV}| \leqslant 4\ \text{keV}$) to the total area of the photo-peak, indicates the fraction of positrons annihilating with the higher momentum electrons. The CDBEPAR the spectrum for 32 h milled sample has been analysed by constructing the ratio curve [29] with respect to the CDBEPAR spectrum of a defect free 99.9999% pure Al single crystal.

3. Results and discussion

The XRD spectra of the ZnO samples, obtained after different milling times, are shown in figure 1. Due to mechanical milling the average grain size (figure 2), calculated from Scherer's formula (here the 101 peak of the ZnO spectrum fitted with a Gaussian), reduces continuously from 76 ± 1 nm (as-supplied ZnO) to 25 ± 0.5 nm (32 h grinding). Actually the grain size, i.e. the coherent scattering region (CSR) in a direction parallel to a diffraction plane [30], is related to the inverse of the FWHM of the respective diffraction peak. Therefore, the increase of the FWHM of the diffraction peaks with grinding (milling) time indicates the degradation of the crystalline nature of the material. As evident from figure 2, a significant decrease of grain size has been found after 2 h milling followed by a gradual decrease for subsequent milling. In a similar system, Damonte *et al* [31] found a major decrease in grain size after 1 h milling. The inset of figure 2 represents the variation of the (002) peak position (centroid) towards lower angle with increased grinding, which is due to the increase of c-axis lattice parameter, that, in turn, leads to the generation of strain [32] in the crystal. To identify the relative contribution

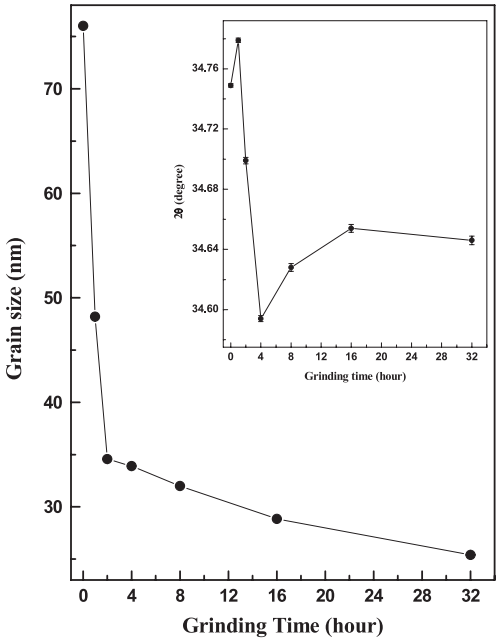

Figure 2. Variation of grain size with grinding time. The inset shows the variation of the (002) peak with grinding time.

of crystallite size and lattice strain in the broadening of the XRD peaks, a Williamson–Hall plot [33], shown in figure 3, has been constructed. The crystallite size and lattice strain can be obtained from the intercept and the slope using the following relation:

$$\beta \cos\theta = (K\lambda/D) + 2\varepsilon \sin\theta$$

where β is the FWHM in radians, D is the average crystallite size, ε is the strain, K is the shape factor, λ is the x-ray wavelength and θ is the Bragg angle. The grain size and strain of the as-supplied samples are found to be ∼90 nm and 5.24×10^{-3} respectively. After 32 h milling, the grain size decreases to ∼39 nm, whereas the strain increases to 12.06×10^{-3}. Although the strain is doubled for the highest milling time it is understood that the strain contribution to the XRD peak broadening is negligible compared to that arising from finite particle size [34].

As evident from powder XRD spectra of milled samples, we have noticed, in corroborating with similar studies in such systems [35], that a large number of defects are introduced in the system during the reduction of grain size by the ball milling process. Therefore, before illustrating the effect of mechanical milling on optical properties, we must discuss the positron annihilation spectroscopic investigation of the system. The variation of CDBEPAR shape parameter (S parameter) with grain size, shown in figure 4, gives a preliminary idea of the changing defective state of the sample. In general, the increase of S parameter is a signature of higher annihilation probability of positrons with the lower momentum electrons. This occurs when the relative concentrations of defects and voids increase in the material. It is well known that in materials with grain size of a few tens of nanometres the majority of the positrons diffuse to the grain surfaces, which are highly defective in nature [11, 35–37]. Such grain surface regions increase with lowering grain size, causing an increase of S parameter. To identify the nature of defects in the milled samples we have also constructed the ratio curve for the unmilled and ball-milled ZnO of the CDBEPAR spectrum with the CDBEPAR spectra of the

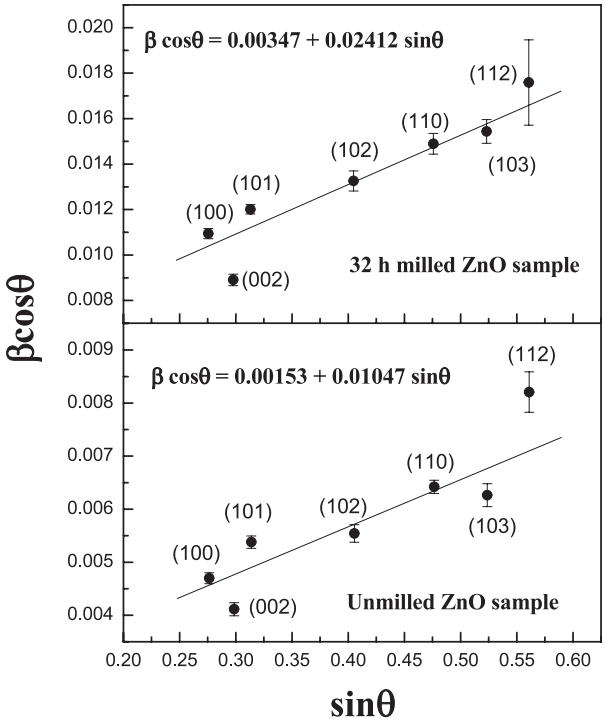

Figure 3. Williamson–Hall plots for unmilled and milled ZnO samples.

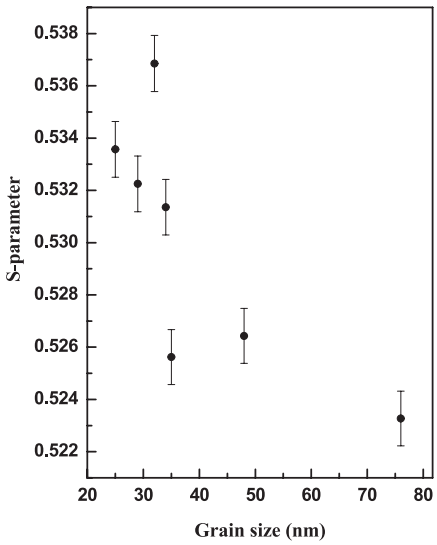

Figure 4. Variation of *S* parameter with grain size for the ZnO samples.

defect free Al single crystals. Figure 5 shows a peak at the momentum value of $\sim 11 \times 10^{-3} m_0 c$ for unmilled and milled samples. Generally, the ratio curves of the oxide materials [29] with respect to Al or Si show a peak near $11 \times 10^{-3} m_0 c$ as the signature of oxygen 2p electrons in

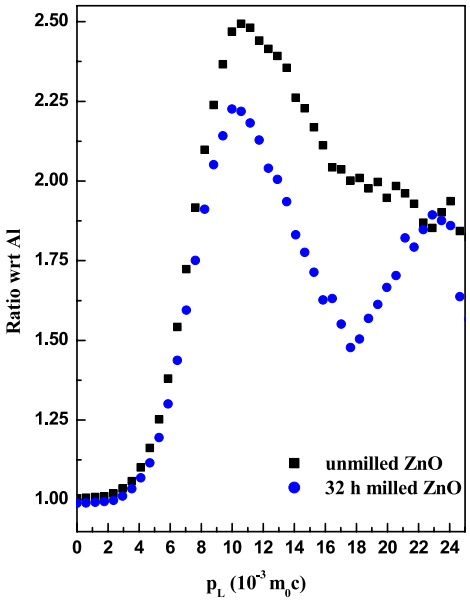

Figure 5. Ratio of the experimental electron–positron momentum distributions for as-supplied and 32 h milled ZnO samples to the electron–positron momentum distributions for the defect free Al single crystal.

the annihilation process. But it has also been observed that in the case of pure Zn when the ratio curve has been constructed with respect to the Al single crystal the same kind of peak has appeared at $11 \times 10^{-3} m_0 c$ [38]. For both unmilled and ball-milled samples, the same kinds of peaks appear but with a lower peak height for the milled one. Also a broad valley is noticeable (figure 5) for both the samples in the momentum range $(15 < p_L < 20) \times 10^{-3} m_0 c$. Such a broad valley in the ratio curve (in the said momentum range) is thought to be a manifestation of complete filling of the 3d and 4s orbitals in zinc [39]. Therefore, we can attribute the peak (figure 5) along with the valley to the reflection of higher positron annihilation with Zn electrons. The lower height of the ratio curve for the milled sample suggests less annihilation of positrons with the electrons of Zn, indicating more Zn vacancy type defects in the sample. To identify the different positron trapping sites, if any, we have also plotted the S-parameter versus W-parameter graph (figure 6), which is a linear one, suggesting only one major trapping site in the system. It should be mentioned here that positrons have a particular affinity to annihilate at the cationic vacancies (here zinc vacancies) in such II–VI semiconducting systems [40]. So oxygen vacancies in ZnO remain more or less invisible to positrons. However, our finding of the Zn vacancy as a dominant defect in ZnO by positron spectroscopy remarkably agrees, as detailed later, with the conclusion from the UV–vis spectroscopic investigation.

At this juncture, we should discuss the effect of milling induced defects and disorder on the optical absorption in ZnO. The spectral absorption coefficient $\alpha(\lambda)$ has been evaluated [11, 35] from the measured spectral extinction coefficient, $k(\lambda)$, using the following expression:

$$\alpha(\lambda) = 4\pi k(\lambda)/\lambda$$

where λ is the wavelength of the absorbed photon. The optical bandgaps (E_g) of the samples have been estimated from the well known expression [41] for direct transition

$$\alpha E = A(E - E_g)^{n/2}$$

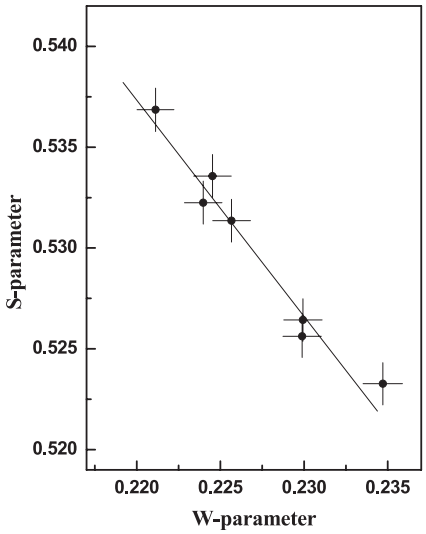

Figure 6. Variation of S parameter with W parameter for unmilled and milled ZnO samples.

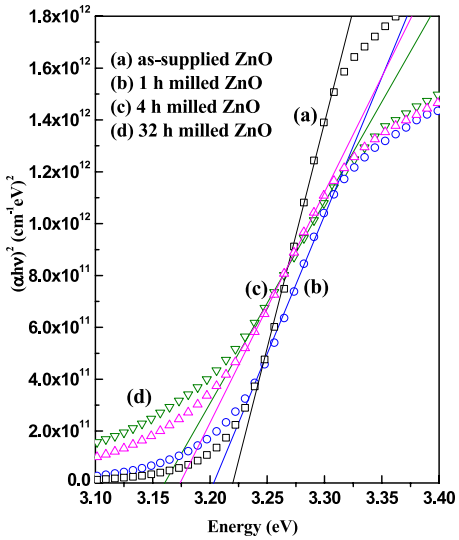

Figure 7. Plots of $(\alpha h\upsilon)^2$ versus photon energy for (a) as-supplied ZnO sample, (b) 1 h ground ZnO sample, (c) 4 h ground ZnO sample, (d) 32 h ground ZnO sample.

where E $(=hc/\lambda)$ is the photon energy and A is a constant. For different values of n, we can try to fit a straight line but a good linearity is observed for $n = 1$, i.e. the direct allowed transition, being the most preferable one in the system studied here. Standard extrapolation of absorption onset [41] to $\alpha E = 0$ (where $E = E_g$) has been shown (figure 7) for selected samples. Small reduction of E_g with lowering of D (average grain size) has been observed. The bandgap value for the non-milled sample with average grain size 76 ± 1 nm is 3.22 eV and that for the 25 ± 0.5 nm sample is 3.15 eV. Such a decrease of bandgap is probably due to the enhanced band bending [42] at grain boundaries. Samples with lower grain size have higher grain surface area, causing more band bending effect. To emphasize, the variation of

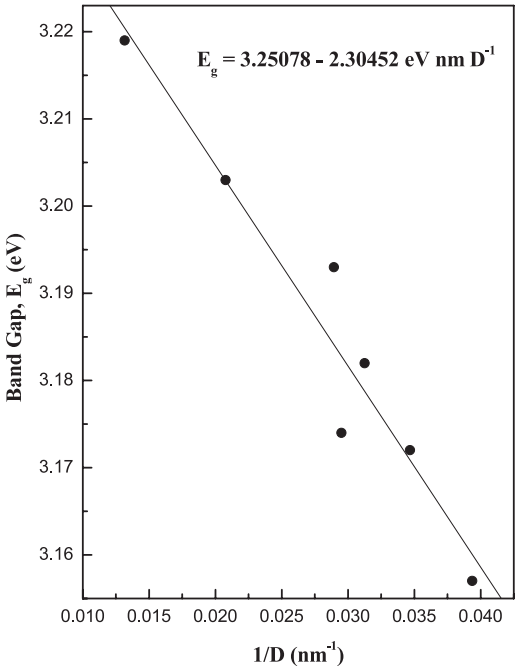

Figure 8. Variation of bandgap with inverse of grain size.

E_g is plotted with the inverse of D (figure 8). A linear relationship with negative slope, which is quite comparable with the coefficient of the Coulomb interaction term [43], can clearly be identified. There exist reports [44] of bandgap enhancement due to quantum confinement in ZnO with grain size similar to that of our samples. However, our findings are just the opposite and are similar to what have been predicted by Srikant *et al* [42] considering the effect of band bending at the grain surface. Probably, in the report of Wang *et al* [44], the heat treatment induced grain growth and a simultaneous occurrence of red-shift in the bandgap (due to the generation of oxygen vacancies [11, 16]) has been attributed to the lowering of bandgap with increasing grain size. As we will see in the next paragraph, the oxygen vacancies affect the optical absorption in ZnO in a different manner from the zinc vacancies.

The effect of overall disorder in such systems is more pronounced in the lower energy tail of the sharp absorption edge indicating the bandgap. An obvious consequence of any disorder is the development of a localization potential [45] that decays with some characteristic length (commonly known as Debye length, L_D [45]), depending on charge carrier concentration, temperature and the static dielectric constant of the medium. A spatially varying electric field is generated inside the material, whose average value is calculated within the grain size. According to the Halperin–Lax model [46], this average value can be linked to the band tailing parameter. However, quantum mechanically, this electric field generates the localized states, which lie within the bulk bandgap of the material. It is to be noted that both the conduction band and the valence band can have tail states inside the bandgap depending on the nature of disorder itself. According to theoretical calculation [41], the absorption coefficient just below the band edge ($E < E_g$) should vary exponentially with absorbed photon energy (E), i.e.,

$$\alpha(E) = \alpha_0 \exp(E/E_0)$$

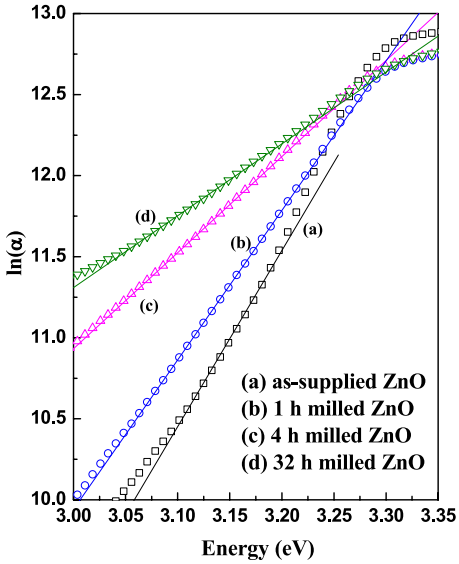

Figure 9. Plots of ln(α) versus photon energy for (a) as-supplied ZnO sample, (b) 1 h ground ZnO sample, (c) 4 h ground ZnO sample, (d) 32 h ground ZnO sample.

where α_0 is a constant and E_0 is an empirical parameter representative of the width of band tail states. E_0 can be estimated from the reciprocal of the slope of the linear part of the ln(α) versus E curve ($E < E_g$), which has been shown in figure 9 for our presently studied ZnO samples. As we have already discussed, the grain boundaries are the source of dominant disorder in nanocrystalline materials; a correlation, therefore, is expected between average grain size (D) and E_0 in these ZnO samples. We have, thus, plotted the relevant data of our other ZnO samples also (which we have studied earlier) in figure 10. Remarkably, all the data points, within the experimental accuracy, follow a simple non-linear behaviour. To note, only the E_0 values of the ZnO samples annealed below 350 °C (earlier samples) follow such a form of variation with the grain size. The relevant values of E_0 for samples annealed higher than 350 °C are scattered and do not follow any particular behaviour. It is well known [11, 16] that above 350 °C annealing oxygen vacancies are generated in large numbers in ZnO. So it can be conjectured at this stage that band tailing in ZnO in the present study (all un-annealed samples) has occurred due to zinc vacancies only. This conforms with the findings from positron spectroscopic investigation. Finally, It is to be mentioned that the grain sizes for our samples are low enough ($\sim$ few tens of nanometres) that an exponential variation is prominent rather than a simple linear relationship with the inverse of the grain size reported in micrometre size CdTe samples [47].

4. Conclusion

We have studied the effect of mechanical milling on structural and optical properties of high purity ZnO by XRD, CDBEPAR and optical absorption spectroscopy. The grain size has been reduced to 25 $\pm$ 0.5 nm (32 h milled ZnO) from 76 $\pm$ 1 nm (as-supplied ZnO) due to milling. The XRD analysis reveals the lowering of grain size as well as generation of strain in ZnO due to milling. The optical absorption spectra of milled samples show red-shift due to increased granular nature. Increase of S parameter indicates an enhancement of defect concentration with lowering grain size. Analysis of the ratio curve for the milled and unmilled samples indicates

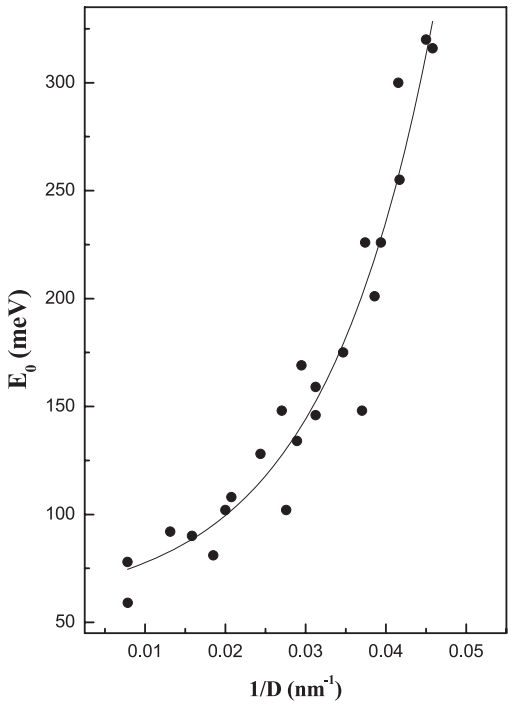

Figure 10. Variation of E_0 with inverse of grain size, fitted exponentially.

the presence of Zn vacancies in the samples. The band tailing parameter (E_0), which has contributions from all possible disorder, also reflects an increase of defects for higher milling time. It has been found that enhanced Zn related vacancy concentration is responsible for such an increase of E_0. Positron annihilation and optical absorption spectroscopy both identify zinc vacancies as a dominant native defect in ZnO.

Acknowledgments

Two of the authors (SD and DJ) are grateful to FIST-DST for providing financial assistance. MS and MC gratefully acknowledge CSIR, Government of India, for providing financial assistance in the form of a fellowship. DJ and AS acknowledge the University Grants Commission, Government of India, for financial help in a minor research project (PSW-029/05-06). The authors are grateful to Professor G N Mukherjee, Department of Chemistry, University of Calcutta, for assistance in acquiring optical data of the samples.

References

[1] Özgür U, Alivov Y I, Liu C, Teke A, Reshchikov M A, Doğan S, Avrutin V, Cho S J and Morkoç H 2005 *J. Appl. Phys.* **98** 041301
[2] Wang Z L 2004 *J. Phys.: Condens. Matter* **16** R829
[3] Look D C 2001 *Mater. Sci. Eng.* B **80** 383
[4] Cao H, Zhao Y G, Ho S T, Seelig E W, Wang Q H and Chang R P H 1999 *Phys. Rev. Lett.* **82** 2278
[5] Meyer B K, Alves H, Hofmann D M, Kriegseis W, Forster D, Bertram F, Christen J, Hoffmann A, Strabburg M, Dworzak M, Haboeck U and Rodina A V 2004 *Phys. Status Solidi* b **241** 231

[6] Tiwari A, Jin C, Narayan J and Park M 2004 *J. Appl. Phys.* **96** 3827
[7] Sundaresan A, Bhargavi R, Rangarajan N, Siddesh U and Rao C N R 2006 *Phys. Rev.* B **74** 161306(R)
[8] Pearton S J, Abernathy C R, Overberg M E, Thaler G T, Norton D P, Theodoropoulou N, Hebard A F, Park Y D, Ren F, Kim J and Boatner L A 2003 *J. Appl. Phys.* **93** 1
[9] Almeida A F L, Fechine P B A, Sasaki J M, Ayala A P, Góes J C, Pontes D L, Margulis W and Sombra A S B 2004 *Solid State Sci.* **6** 267
[10] Jiang J Z, Olsen J S, Gerward L, Frost D, Rubie D and Peyronneau 2000 *J. Europhys. Lett.* **50** 48
[11] Dutta S, Chattopadhyay S, Jana D, Banerjee A, Manik S, Pradhan S K, Sutradhar M and Sarkar A 2006 *J. Appl. Phys.* **100** 114328
[12] Matsumoto T, Kato H, Miyamoto K, Sano M, Zhukov E A and Yao T 2002 *Appl. Phys. Lett.* **81** 1231
[13] Tobin G, McGlynn E, Henry M O, Mosnier J P, Lunney J G, O'Mahony D and dePosada E 2003 *Physica* B **340–342** 245
[14] Shalish I, Temkin H and Narayanamurti V 2004 *Phys. Rev.* B **69** 245401
[15] Zubiaga A, Garcia J A, Plazaola F, Tuomisto F, Saarinen K, Pérez J Z and Muñoz-Sanjosé V 2006 *J. Appl. Phys.* **99** 053516
[16] Dutta S, Chakrabarti M, Chattopadhyay S, Sanyal D, Sarkar A and Jana D 2005 *J. Appl. Phys.* **98** 053513
[17] Chichibu S F, Onuma T, Kubota M, Uedono A, Sota T, Tsukazaki A, Ohtomo A and Kawasaki M 2006 *J. Appl. Phys.* **99** 093505
[18] Lee J, Gao W, Li Z, Hodgson M, Metson J, Gong H and Pal U 2005 *Appl. Phys.* A **80** 1641
[19] Ozerov I, Nelson D, Bulgakov A V, Marine W and Sentis M 2003 *Appl. Surf. Sci.* **212–213** 349
[20] Tan S T, Chen B J, Sun X W, Hu X, Zhang X H and Chua S J 2005 *J. Cryst. Growth* **281** 571
[21] Cho S, Ma J, Kim Y, Sun Y, Wong G K L and Ketterson J B 1999 *Appl. Phys. Lett.* **75** 2761
[22] Tang Z K, Wong G K L, Yu P, Kawasaki M, Ohtomo A, Koinuma H and Segawa Y 1998 *Appl. Phys. Lett.* **72** 3270
[23] Zhang Y, Lin B, Sun X and Zhuxi F 2005 *Appl. Phys. Lett.* **86** 131910
[24] Urbieta A, Fernández P and Piqueras J 2004 *J. Appl. Phys.* **96** 2210
[25] Radoi R, Fernández P, Piqueras J, Wiggins M S and Solis J 2003 *Nanotechnology* **14** 794
[26] Cullity B D 1978 *Elements of X-ray Diffraction* (Philippines: Addison-Wesley)
[27] Lynn K G and Goland A N 1976 *Solid State Commun.* **18** 1549
[28] Chakraborti M, Sarkar A, Chattopadhayay S, Sanyal D, Bhattacharya R, Pradhan A K and Banerjee D 2003 *Solid State Commun.* **128** 321
[29] Chakrabarti M, Sarkar A, Sanyal D, Karwasz G P and Zecca A 2004 *Phys. Lett.* A **321** 376
[30] Jejurikar S M, Banpurkar A G, Limaye A V, Date S K, Patil S I, Adhi K P, Misra P, Kukreja L M and Bathe R 2006 *J. Appl. Phys.* **99** 014907
[31] Damonte L C, Mendoza Zélis L A, Mari Soucase B and Hernández Fenollosa M A 2004 *Powder Technol.* **148** 15
[32] Yadav T P, Mukhopadhyay N K, Tiwari R S and Srivastava O N 2005 *Mater. Sci. Eng.* A **393** 366
[33] Williamson G K and Hall W H 1953 *Acta Metall.* **1** 22
[34] Tan S T, Chen B J, Sun X W, Fan W J, Kwok H S, Zhang X H and Chua S J 2005 *J. Appl. Phys.* **98** 013505
[35] Chakrabarti M, Dutta S, Chattopadhyay S, Sarkar A, Sanyal D and Chakrabarti A 2004 *Nanotechnology* **15** 1792
[36] Dupasquier A and Somoza A 1995 *Mater. Sci. Forum* **175–178** 35
[37] Thakur V, Shrivastava S B and Rathore M K 2004 *Nanotechnology* **15** 467
[38] Ghosh V J, Alatalo M, Asoka-Kumar P, Nielsen B, Lynn K G, Kruseman A C and Mijnarends P E 2000 *Phys. Rev.* B **61** 10092
[39] Brusa R S, Deng W, Karwasz G P and Zecca A 2002 *Nucl. Instrum. Methods Phys. Res.* B **194** 519
[40] Plazaola F, Seitsonen A P and Puska M J 1994 *J. Phys.: Condens. Matter* **6** 8809
[41] Pancove J 1979 *Optical Processes in Semiconductors* (Englewood Cliffs, NJ: Prentice-Hall)
[42] Srikant V and Clarke D R 1997 *J. Appl. Phys.* **81** 6357
[43] Brus L 1986 *J. Phys. Chem.* **90** 2555
[44] Wang Y G, Lau S P, Lee H W, Yu S F, Tay B K, Zhang X H and Hng H H 2003 *J. Appl. Phys.* **94** 354
[45] Smith R A 1964 *Semiconductors* (Cambridge: Cambridge University Press)
[46] Halperin B I and Lax M 1966 *Phys. Rev.* **148** 722
[47] Iribarren A, Castro-Rodríguez R, Sosa V and Peña J L 1999 *Phys. Rev.* B **60** 4758